Carbohydrate Polymers 245 (2020) 116530

Contents lists available at ScienceDirect

Carbohydrate Polymers

journal homepage: www.elsevier.com/locate/carbpol

Synthesis of chitosan-based flame retardant and its fire resistance in epoxy resin

Rui Chen[a,b], Zijin Luo[a], XueJun Yu[c], Hao Tang[a], Yuan Zhou[a], Hong Zhou[a,*]

[a] Wuhan Institute of Technology, Wuhan, 430073, China
[b] West Anhui University, Lu'an, 237012, China
[c] Three Gorges Public Inspection and Testing Center, Yichang, 443000, China

ARTICLE INFO

Keywords:
Epoxy resin
Flame-retardant
Chitosan
DOPO

ABSTRACT

A novel flame retardant CCD was synthesized by the condensation between cinnamalde and chitosan, followed by the addition reaction with 9,10-dihydro-9-oxa-10-phosphaphenanthrene-10-oxide(DOPO), and CCD was named from the initials of the three raw materials. The intermediate product CC and the target product CCD was then characterized by infrared spectrometry and elemental analysis. The flame retardancy of EP thermosets modified by CCD was dramatically improved. Epoxy resin (EP) with 10wt% CCD passed vertical burning (UL-94) V-0 rating and possessed limited oxygen index (LOI) value of 31.6 %. Cone calorimeter test exhibited the introduction of 3.5g CCD into 35g EP decreased the total heat release by 38.8 % and decreased the total smoke product by 72.0 %. XPS, FTIR, SEM and Raman tests were proceeded to determine the char residue for EP/10 % CCD thermoset, and the results showed that char residue for EP/10 % CCD thermoset possessed dense and compact structure which played a positive effect in blocking the exchange of heat and gas.

1. Introduction

Epoxy resin, one of the most advanced thermoplastic resins, has been widely applied in various fields of industrial production such as adhesives (Rakotomalala, Wagner, & Döring, 2010), surface coating materials, molding compounds, printed circuit boards and microelectronic materials. However, the utilization of epoxy resin is severely limited by its inherent combustibility (Mariappan & Wilkie, 2014). Therefore, in order to make full use of its outstanding advantages such as low shrinkage, good adhesion, good chemical corrosion resistance and high mechanical strength, the improvement for the flame retardancy of epoxy resin is an imperative research topic (Zhao, Babu, Llorca, & Wang, 2016).

Chitosan is a natural polysaccharide composed of amino-containing 2-deoxyglucan. This linear polysaccharide is produced from chitin by its alkaline deacetylation. Due to its widespread accessibility, non-toxicity, compatibility, biodegradability and low price, chitosan had been widely utilized in biotechnology, biomedical engineering, wastewater treatment, food and cosmetic processing (Shen, Xu, Long, Shi, & Chen, 2017), since it was discovered in 1859. It had been reported that chitosan was a hopeful and promising green charring agent, because of the exsistence of multi-hydroxyl and multi-amino groups in its structure. Besides, it had been reported that chitosan derivatives (Yang, Wang, Huo, Wang, & Tang, 2016) had been directly utilized as a charring agent in flame retardant composite. In their work, chitosan was modified by reacting with benzaldehyde, hydroxybenzaldehyde and salicylaldehyde and three different chitosan derivatives (Liu, Gu, Sun, & Zhang, 2017) were successfully synthesized, respectively. Unfortunately, all these chitosan derivatives did not have flame retardancy independently. In order to improve flame retardancy, ammonium polyphosphate (APP) was then introduced into thermoplastic polyurethane(TPU)/ chitosan derivative composites. For example, the composite containing 18.75 wt% APP and 6.25 wt% salicylaldehyde modified CS (SCS) passed the V-0 rating with the maximal limiting oxygen index of 29.5 %. The large additive amount of APP was likely to reduce the mechanical strength of composites. Besides, the large amount of phosphorus generated from combustion was proposed to cause eutrophication of the water.

DOPO which had been widely applied to develop flame-retarding epoxy resin, was regarded as the most promising raw material to design new flame retardant additives by making use of the high reactivity of P—H bond (Zang, Wagner, Ciesielski, Müller, & Döring, 2011). The active PH bond in the DOPO reacted with CN bond in Schiff-base compounds (—═Tang, Zhu, Chen, Wang, & Zhou, 2019), therefore, a lot of flame retardant additives based on Schiff-base and DOPO were been designed and synthesized in recent years. Unfortunately, DOPO

* Corresponding author.
E-mail address: hzhouh@126.com (H. Zhou).

https://doi.org/10.1016/j.carbpol.2020.116530
Received 15 March 2020; Received in revised form 29 April 2020; Accepted 27 May 2020
Available online 03 June 2020

did not have enough activity to react with C═N bond derived from aldehydes and amino group in chitosan. In addition, DOPO was also active to C═C bond. A flame retardant named ABD (Jin, Qian, Qiu, Chen, & Xin, 2019) was synthesized via addition reaction between acrolein and DOPO. Then, ABD with the structure of relatively short bonds, a hydroxyl group and two DOPO residues was introduced into epoxy resin, and exhibited perfect fire resistance. When the introduction of ABD was only 3 wt%, the thermoset passed V-0 rating with the maximal limiting oxygen index of 36.2 %. Similarly, cinnamaldehyde was yellow sticky aldehyde and had the structure of an acrolein attached to a phenyl group. The aldehyde group of cinnamaldehyde was proposed to react with the amino group of chitosan, and C═C bond of cinnamaldehyde was proposed to combine with DOPO.

The goal of this work was to prepare environmental friendly flame retardant epoxy resin which reduced uttermostly the disadvantages of epoxy resins materials for sustainable development. The novel flame retardant CCD based on chitosan, DOPO, and cinnamaldehyde was designed and synthesized. Then, the flame-retardant EP thermosets modified by CCD were prepared. The thermal properties of flame- retardant EP/CCD thermosets were tested by thermogravimeric analysis (TGA), differential scanning calorimeter (DSC). Flame-retardant properties of EP/CCD thermosets were analyzed by LOI, UL-94 and cone calorimeter test.

2. Experimental

2.1. Materials

Diglycidyl ether of bisphenol A (DGEBA, E-44) was purchased from Nantong Xingchen Synthetic Material Co., Ltd. (Nantong, China.). DOPO was provided by Eutec Trading (Shanghai) Co., Ltd. Cinnamaldehyde, 4,4′- Diaminodiphenyl methane (DDM) and chitosan with a deacetylation degree of 95 % was offered by Aladdin Chemistry (Shanghai) Co., Ltd., ethanol was purchased from Sinopharm Chemical Reagent Co., Ltd. used without further purification.

2.2. Synthesis of CCD

CCD was prepared by a two-step synthetic method, as described in Fig. 1. Firstly, the intermediate CC was synthesized by a typical condensation reaction. Specifically, 8.10 g (equivalent to 0.05 mol -NH_2) chitosan was added to a 250 mL round flask, and then the reactor was equipped with and a reflux condenser a magnetic stirrer. Subsequently, 0.07 mol cinnamaldehyde dissolved in 100 mL ethanol was poured into the reactor, and the mixture was refluxed at 60 ℃ and for 24 h. After cooling to room temperature, the intermediate CC in the mixture was filtered and then washed with ethanol for three times to remove redundant cinnamaldehyde. The intermediate CC was dried at 55 ℃ for 24 h.

Secondly, the product CCD was obtained through the nucleophilic addition reaction between DOPO and the intermediate CC. Specifically, a 250 mL round flask equipped with a reflux condenser and a magnetic stirrer was charged with 100 mL ethanol, the intermediate CC and DOPO (15.2 g, 0.07 mol). The reaction mixture was stirred at 60℃. 4 h later, the solvent was removed, the target product CCD was obtained and was poured into ethanol to be further purified. Finally, the solid was filtered, and dried at 55 ℃ for 24 h with the help of vacuum (Yang, Wang, Huo, Cheng, & Wang, 2015).

2.3. Preparation of flame-retarded epoxy resins

Flame retarded thermosets EP/CCD were prepared and the formulations for CCD/DDM/EP system were listed in Table 1. Firstly, CCD and epoxy resins were added to a glass reactor, and the mixture was stirred at 90 ℃ with the help of vacuo. 5 min later, the mixture turned into homogeneous mixture. Then, DDM was added into the homogeneous mixture and the mixture was further mingled for 5 min. Finally, the homogeneous mixture was quickly fed into PTFE moulds. Flame retarded thermosets EP/CCD were cured at 100 ℃ for 2 h and subsequently at 150 ℃ for 3 h. The control group was EP thermoset prepared under the same processing conditions without CCD (Schartel, Balabanovich, Braun, Knoll, & Artner, 2007).

2.4. Characterization

Fourier transform infrared (FT-IR) spectrum of CCD and the char residue for EP/CCD were analyzed by the Thermo Nicolet 5700 FT-IR spectrophotometer using KBr disk, and the wavenumber was in the range of 400 cm^{-1}–4000 cm^{-1}.

Vario MACRO cube elemental analyzer was used to analyze the

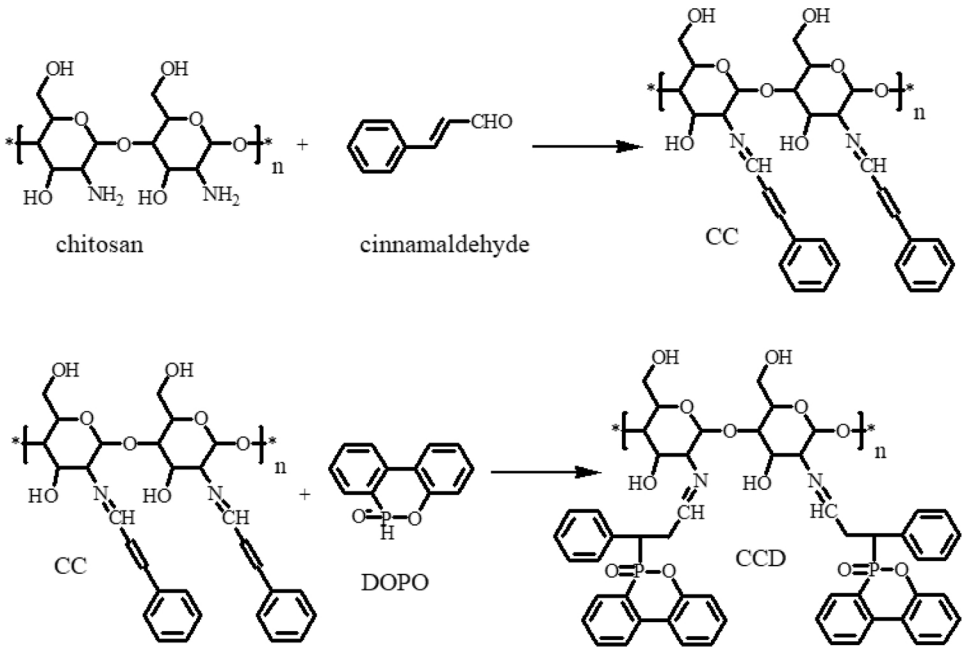

Fig. 1. Synthetic route of CCD.

Table 1
formulations of the flame-retarded epoxy resins.

sample	EP (g)	DDM(g)	CCD (g)	UL94(3.2 m)	LOI(%)
EP	25.0	6.50	0	N.R	25.8
EP/6 % CCD	25.0	6.50	2.01	V-1	29.2
EP/8 % CCD	25.0	6.50	2.74	V-1	30.5
EP/10 % CCD	25.0	6.50	3.50	V-0	31.6

content of C, H and N in chitosan and its derivatives (Xiong, Jiang, Xie, Zhang, & Xu, 2013).

DSC analysis of EP/CCD thermosets was carried out on a TAQ200 DSC (TA, USA). Glass transition temperatures (Tg) of the thermosets were determined from 40 ℃ to 300 ℃ with the heating rate of 10 ℃/min under nitrogen atmosphere. TGA was recorded on by Netzsch 2209F1 thermo-gravimetric analyzer under nitrogen atmosphere from 30 ℃ to 800 ℃. The sample of about 15 mg was used in each measurement, which was placed on open oven at a heating rate of 10 ℃/min (Gao & Yang, 2010).

According to ASTM D2863－97, limiting oxygen index (LOI)was tested on oxygen index instrument made in UK (Fire Testing Technology Co., Ltd) and the dimension of EP/CCD thermosets was 150 × 6.5 × 3.2 mm^3. According to ASTM D3801, vertical burning test was performed on UL 94 flammability meter made in UK (Fire Testing Technology Co. Ltd.) and the dimension was 130 × 13 × 3.2 mm^3. The samples were held 10 cm over the burner and rapidly removed after exposure to outer flame for 10 s. Cone calorimeter test was carried out according to ISO5660 by FTT cone calorimeter made in UK. The EP/CCD thermosets dimension was 100 × 100 × 5 mm^3 under an external heat flux of 35 kW/m^2 (Buczko, Stelzig, Bommer, Rentsch, & Heneczkowski, 2014).

The elements state of char residues was analyzed by X-ray photoelectron spectrometer made in USA(Thermo fisher Scientific Co.) with a Al Ka excitation radiation (hv = 1486.6 eV) under high vacuum conditions (Dong, Deng, Li, Cao, & Lin, 2016).

The morphologies of char surfaces after combustion were detected by a JEOL JSM-5900LV SEM under an accelerating voltage of 20 kV (Shao, Deng, Tan, Chen, & Chen, 2014).

Raman spectroscopy used to characterize the types of the carbon was LabRAMHR800 laser Raman spectrometer (SPEX Co.). The operation was carried out at room temperature under 532 nm helium-neon laser line (Yang, Xu, & Li, 2013).

3. Results and discussion

3.1. Structure characterization of CCD

The FTIR spectra of chitosan and its derivatives CC and CCD were shown in Fig. 2. In the FTIR spectrum of chitosan, characteristic peaks at 1156 cm^{-1} and 1602 cm^{-1} were observed. These stretching vibration were assigned to the saccharide structure and amino groups. In the FTIR spectrum of CC, The new stretching vibration for −CN at 1632 cm^{-}=$-^{1}$ was detected which demonstrated that amino groups in chitosan had been completely reacted with cinnamaldehyde. Moreover, additional characteristic peaks at 750 cm^{-1} was assigned to phenyl groups in the intermediate product CC. Characteristic stretching vibration for −CC at 687 cm^{-}=$-^{1}$ further conformed the structure of intermediate product CC. In the FTIR spectrum of chitosan, the characteristic absorption signal at 687 cm^{-1} was disappeared, providing that the introduction of DOPO completely converted CC into CC.−=−−−− Meanwhile, the characteristic stretching vibration at about 1632 cm^{-1} was observed in CCD indicating that CN was not active enough to react with DOPO(−=−Dong, Deng, & Wang, 2017).

The chemical structures of CC and CCD were further verified by elemental analysis. The contents of C, N, and H atoms of chitosan and its derivatives were also detected and the corresponding data were exactly presented in Table 2. In Table 2, the content of C in chitosan was 44.62 %, while the contents of C in chitosan derivatives were 66.31 % and 66.16 %, respectively. The reduction in nitrogen is the most marked in all elements. It descended from 8.15 % in chitosan to 2.96 % in CD due to the introduction of nitrogen-free groups cinnamaldehyde and DOPO. Moreover, there were also significant changes in the H content of chitosan and its derivatives. The result of elemental analysis of chitosan and its derivatives further confirmed that its derivatives CC and CCD were successfully synthesized.

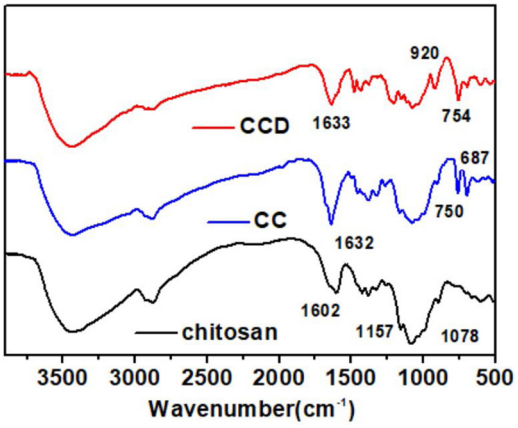

Fig. 2. FTIR spectra of CC and CCD.

Table 2
elemental analysis data of chitosan and its derivatives.

elemental sample	C	N	H
chitosan	44.62	8.15	6.72
CC	66.31	5.11	5.88
CCD	66.16	2.96	5.13

3.2. Thermal analysis

The glass transition temperatures (Tg) of epoxy resin thermosets modified with chitosan derivative CCD were detected by DSC test. As shown in Fig. 3(a), it was obviously seen that the neat epoxy resin thermoset had the highest Tg value of 158.7 ℃. With the introduction of the flame retardant additive CCD, the Tg values of EP/CCD thermosets decreased dramaically. Glass transition temperatures (Wang, Hu, Song, Xing, & Lu, 2011) for EP/6 % CCD decreased to 148.9 ℃, which was nearly 10 ℃ lower than the transition temperature of pure EP thermoset. With the increase of additive amount of CCD, the glass transition temperatures further decreased. For example, the glass transition temperature of EP/8 % CCD was 144.1 ℃, while EP/10 % CCD reached 140.7 ℃, respectively. EP/CCD thermosets was believed to possess lower cross-linking density and thus the lower glass transition temperatures. As a DOPO-based chitosan derivative, CCD was presumed to reduce the cross-linking density of epoxy resin.

Thermal gravimetric analysis (TGA) was utilized to detect the thermal behavior of thermosets by using a Netzsch 2209F1 instrument under nitrogen atmosphere. The TGA curves of the control group and EP samples modified by CCD were displayed in Fig. 3(b). The TGA curve of the control group EP thermoset was one-step degradation process while EP/CCD thermosets possessed similar weight-loss processes (Zhao, Liu, Peng, Liao, & Wang, 2015). The control group EP thermoset had the highest $T_{5\%}$ of 355.6 ℃, on the contrary, its T_{max} at 380.5 ℃ was the lowest of all thermosets. With the introduction of 10 % CCD, the $T_{5\ \%}$ of EP/10 % CCD thermoset decreased to 341.3 ℃. It was obvious that the T_{max} of EP/CCD thermosets ranged from 395.1 ℃ to

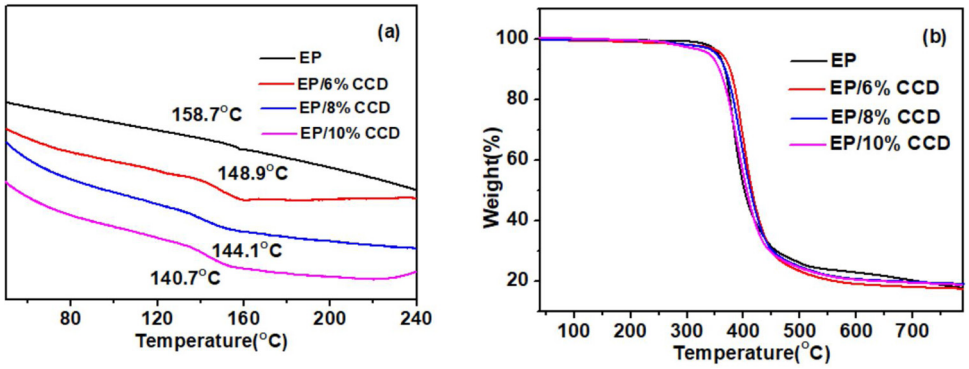

Fig. 3. DSC curves(Fig. 3(a)) and TGA curves(Fig. 3(b)) of EP and EP/CCD.

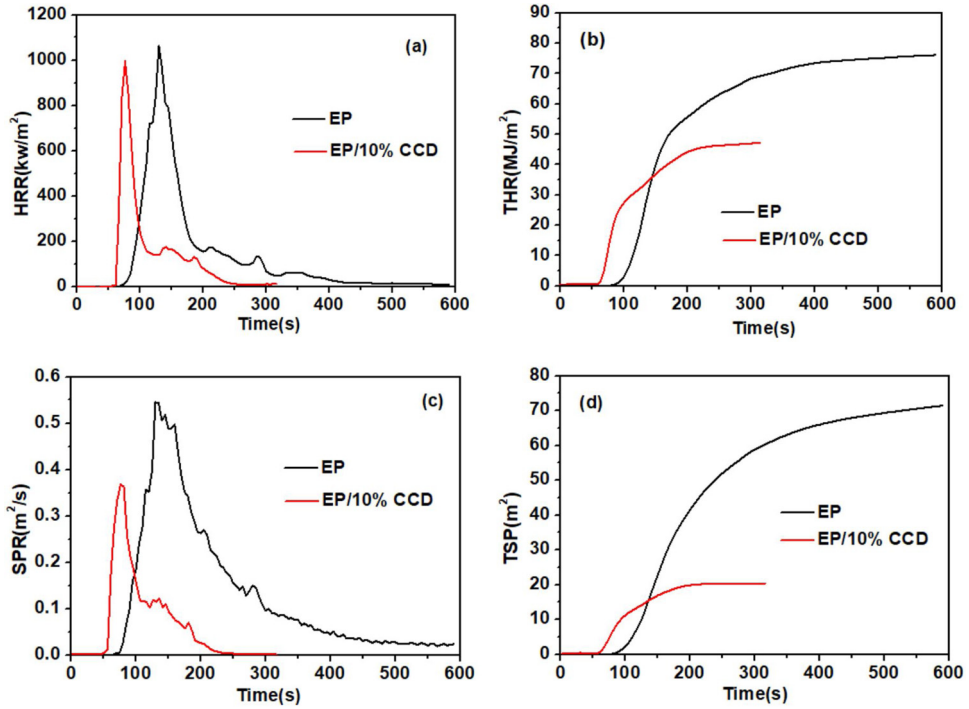

Fig. 4. The curves of HRR, THR, SPR and TSP of neat EP and EP/6 % CCD.

Table 3
The Cone calorimeter test results of neat EP and EP/6 % CCD thermoset.

Sample	EP	EP/10 % CCD
Time for ignition(s) (TTI)	59	55
Time to peaks(s) (t_p)	130	75
Peak heat release rate (kW/m^2) (PHRR)	1063.1	997.1
fire growth rate index (FIGRA)	8.17	7.41
Total heat release (MJ/m^2) (THR)	76.1	46.6
Peak smoke produce rate (m^2/s) (PSPR)	0.54	0.36
Total smoke release (m^2) (TSP)	71.4	20.1
Average effective combustion heat (MJ/kg)	13.4	18.3
Average CO yield (kg/kg) (AV-COY)	0.054	0.084
Average CO_2 yield (kg/kg) (AV-CO2Y)	0.995	1.151
Char residue (%)	11.9	15.4

390.7 ˚C showed a declining trend with the additive amount of CCD increased. The char residue under nitrogen atmosphere at 800 ℃ of EP thermosets increased from 17.42 % for the control group to 22.52 % for EP/10 % CCD thermoset.

3.3. LOI and UL94 vertical burning tests

In order to assess the flame retardancy of chitosan derivative CCD, the combustion properties of EP and EP/CCD thermosets were detected by LOI and vertical burning tests. Table 1 exactly showed that, the LOI of neat EP thermoset was 25.8 %, which was the lowest in the tested thermosets. However, the introduction of chitosan derivative CCD significantly improved flame retardancy of EP thermoset. As shown in Table 1, the LOI value was increased from 29.2 % for EP/6 % CCD to 31.6 % for EP/10 % CCD. In respect of UL-94 test, EP/10 % CCD thermoset passed V-0 rating, while EP/6 % CCD thermoset and EP/8 % CCD thermoset reached V-1 rating. The control group was the most combustible in the samples and failed in vertical burning tests with serious burning drips. In terms of burning time, the flame of EP/10 % CCD thermoset spontaneously extinguished much earlier than the other thermosets (Wang, Ma, Wang, Qiu, & Cai, 2018). All the data in LOI and UL94 vertical burning tests demonstrated that chitosan derivative CCD possessed perfect flame retardancy.

3.4. Cone calorimeter test

Cone calorimeter test offered more specific information for the

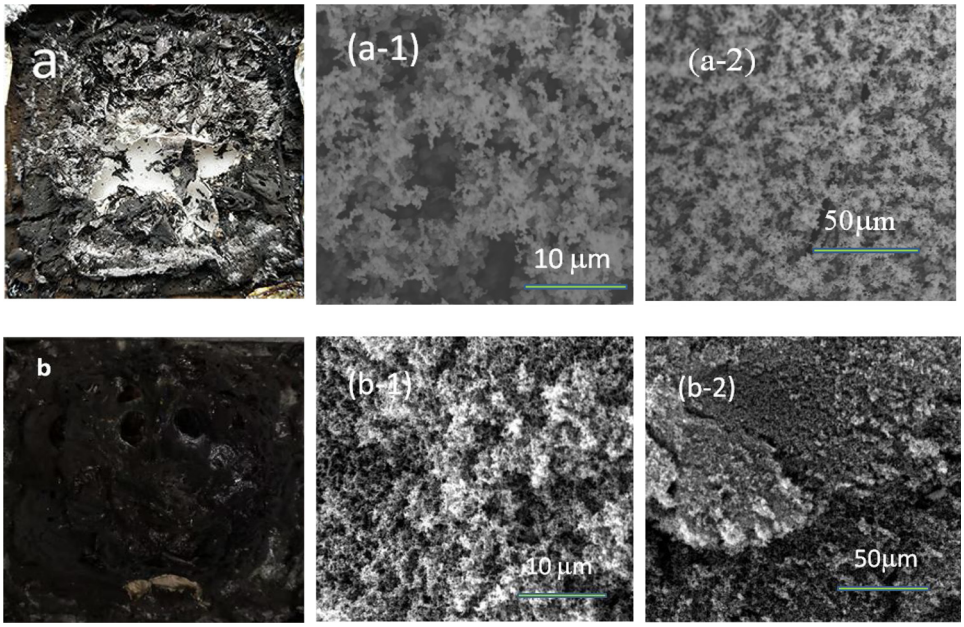

Fig. 5. Digital and SEM images of char residues for EP (a) and EP/6 % CCD (b).

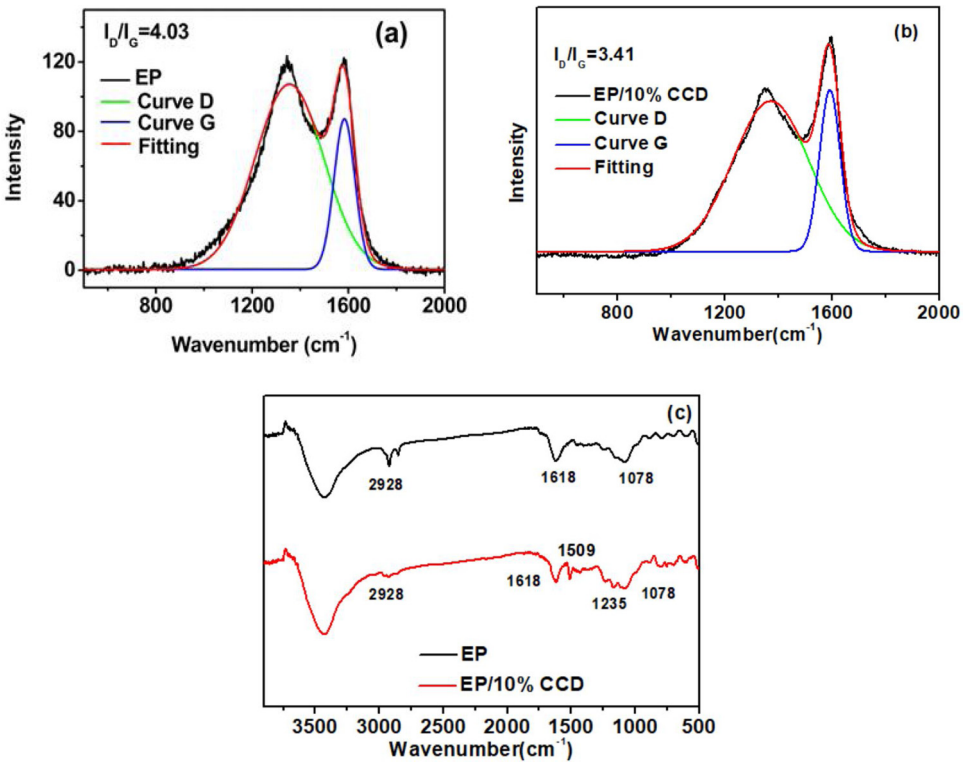

Fig. 6. Raman and FT-IR spectrum of char residues for EP and EP/10 % CCD.

combustion behaviors of neat EP and EP/10 % CCD thermosets, for example, the time for ignition, heat release, smoke production and gas release. In respect of the time for ignition (TTI), the TTI for EP/10 % CCD was 55 s, while the TTI for the control group was 59 s. The shorter TTI for EP/10 % CCD was consistent with the data of thermal gravimetric analysis, which indicated earlier decomposition of CCD. Due to earlier decomposition of CCD, EP/10 % CCD exhibited the earlier behavior of releasing heat. As shown in Fig. 4(a) and (b). heat release rate (HRR) and total heat release (THR) of EP/10 % CCD appeared earlier than relative ones of neat EP thermoset. It was seen that the introduction of chitosan derivative CCD dramatically depressed total heat release. Fig. 4(c) and(d) was smoke produce rate (SPR) and total smoke release (TSP) for EP and EP/10 % CCD thermosets. The trend of smoke release was basically analogous to heat release. It was obviously that the total smoke release for EP/10 % CCD was less than a third of the total smoke release of the control group.

The other data such as the time to peak (t_P), average of effective heat of combustion (av-EHC), average CO yield (AV-COY), average CO_2 yield (AV-CO2Y), and the yields of the char residue were enumerated in Table 3.

In terms of neat EP thermoset, the combustion of neat EP thermoset reached the summit at 130 s. The average effective combustion heat

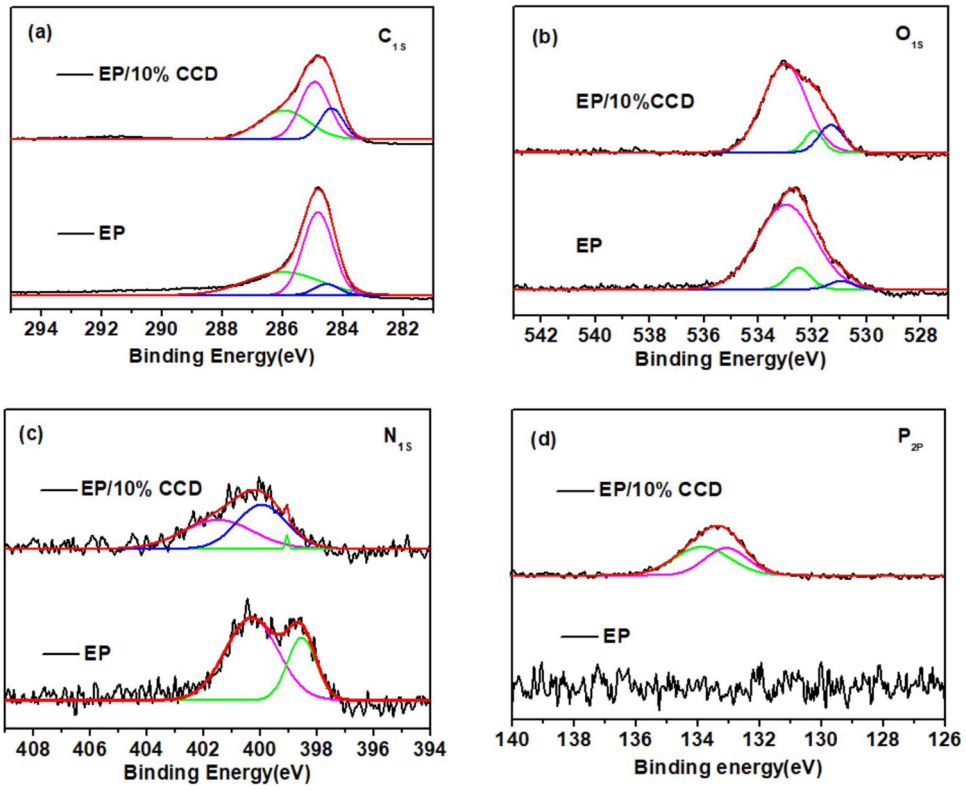

Fig. 7. XPS spectrum of char residues for EP and EP/10 % CCD.

(Av-EHC) was 13.4 MJ/kg which meant that abundant heat was generated by the combustion of the material, and the heat improved further combustion of the inner material. AV-COY and AV-CO2Y was 0.054 kg/kg and 0.995 kg/kg, respectively.

Compared with neat EP thermoset, the time to peak of EP/10 % CCD was at 75 s, which was only 20 s after TTI of EP/10 % CCD. Av-EHC of EP/10 % CCD was 18.3 MJ/kg, while AV-COY and AV-CO2Y of EP/10 % CCD increased to 0.084 kg/kg and 1.151 kg/kg, respectively. Considering the combustion time of the experiment, the total CO yield and CO_2 yield was decreased. The char residue for EP/10 % CCD was 15.4 %, which was 129 % the of the control group. The increase of the char residue for EP/10 % CCD was consistent with the result of thermal gravimetric analysis.

3.5. Char residues analysis

Fig. 5(a, b) was the digital photos of char residues from cone calorimeter tests for EP thermoset and EP/10 % CCD thermoset. The char residue for neat EP thermoset was loose and fragmentary indicating the weak charring ability of EP independently, while more char residue was formed from EP/10 % CCD thermoset. The homogeneous char residue implied that the introduction of CCD facilitate char forming in residue. The char residues generated from of EP thermoset and EP/10 % CCD thermoset were further analyzed by SEM. Fig. 5 (a-1,a-2) was the images of the char residue for neat EP thermoset. It was loose and broken with many holes. Compared with EP thermoset, EP/10 % CCD had more compact and more cross-linked structure.

In order to obtain more information of char residues for EP and EP/10 % CCD after combustion, the char residues for EP/10 % CCD thermoset after cone calorimeter test was further investigated by Raman spectroscopy (Jian, Wang, Xia, Yu, & Zheng, 2017). Fig. 6(b) was Raman spectra of residue for EP/10 % CCD thermoset and Fig. 6(a) was the control group. As exhibited in control group, there were two peaks in the spectra, which belonged to D (1369 cm^{-1}) and G (1592 cm^{-1}) bonds respectively. As we know, the peak at 1369 cm^{-1} represented amorphous carbon, corresponded to disordered carbon or graphite, while the other generated from absorption peak of the sp^2-hybridized carbon atoms. The graphitization degree of the char was measured by proportion of the integrated intensities of the two peaks. The lower proportion of ID/IG represented the relatively higher graphitization of char residue after combustion, and the higher graphitization was helpful to flame retardancy in condensed-phase (Zhu, Xu, Liao, Xu, & Wang, 2017). Raman spectrum showed that, the peak at 1592 cm^{-1} in EP/10 % CCD was higher than the peak in control group and the proportion of ID/IG of the residue for EP/10 % CCD was 3.41, which was much smaller than the value of control group (4.03). The result of Raman spectrum indicated that the char residue of EP/10 % CCD was consisted of graphite-like complexes. The compact graphite-like complexes inhibited the transfer of gas and mass better, and in the end, offered better protection for inner thermoset. The Raman spectrum of char residues accorded with the results of SEM.

Moreover, the char residues for the control group and EP/10 % CCD thermoset were further analyzed by FTIR. As shown in Fig. 6(c), the vibration of O—H and NH— bonds at about 3440 cm^{-1} was the most obvious, indicating that the char residues were composed of hydroxy compounds and ammonium compounds. Besides, characteristic absorption peaks of char residue for control group were at 2928 cm^{-1}, 1618 cm^{-1} and 1078 cm^{-1}. These three characteristic absorption peaks were ascribed to vibration of aromatic rings indicating that the residue for the control group contained enormous aromatic compounds. In Fig. 6(c), the peak evoked by vibrations of P—C at 1509 cm^{-1} was found in FTIR spectra of char residue for EP/10 % CCD, and this peak was the most obvious difference between the IR spectrum of char residue for EP thermoset and char residue for EP/10 % CCD thermoset. Moreover, the stretching vibrations of P═O at 1235 cm^{-1} was also observed, but the peak of P—OC— was not conspicuous. These characteristic absorption peaks determined that the main combustion product of EP/10 % CCD was rich in aromatic compounds, and the phosphorus in the char residue was mainly in the form of PC and PO—═.

The status of C, N, O and P in the char residue for EP thermoset and

EP/10 % CCD thermoset was further analyzed by XPS and the results of XPS spectrum were showed in Fig. 7. Fig. 7(a) was C_{1s} spectrum for the char residues of EP thermoset and EP/10 % CCD thermoset. Both the control group and EP/10 % CCD had only one peak at about 284.8 eV in C_{1s} spectrum, indicating that the major carbon in char residue was in form of C−C and CH (−Liang, Zhao, Zhao, Zhang, & Liu, 2017). Besides, the asymmetry of Fig. 7(a) was due to C−O bonds at 285.9 eV and C═O bonds at 287.9 eV. The subtle difference between C_{1s} spectrum of the char residue for EP thermoset and EP/10 % CCD thermoset was ascribed to the PC− bond generated from combustion. As shown in Fig. 7b, O_{1s} spectrum of EP and EP/10 % CCD had peak at about 532.8 eV indicating that the major oxygen in char residue was in form of C−OC, COP and POP−−−−− (533 eV). O_{1s} spectra of the control group had better symmetry, while O_{1s} spectra of the char residue for EP/10 % CCD had the inflection point at 531.2 eV which was ascribed to P═O bond (Zhu, Wang, Dong, Liao, & Wang, 2019). In N_{1s} spectrum of the char residue of EP, two peaks at 398.7 eV and 400.5 eV were observed, which was belonged to C−N bond and NH− bond, respectively. The introduction of flame retardancy CCD produced absorption peak at 399.8 eV which was due to N–P bond in char residue, and further changed the N_{1s} spectra of residue into asymmetric unimodal curve. Fig. 7d exhibited P2p spectrum of the char residue for EP and EP/10 % CCD, the characteristic peak in spectra of the char residue for EP/10 % CCD at 133.6 eV was ascribed to P−O (133.5 eV) and PO═ (134.2 eV).

4. Conclusion

In this work, a novel flame retardant additive based on chitosan and DOPO, named CCD, was successfully synthesized. The introduction of CCD dramatically improved the flame retardancy of EP. Flammability properties testing of EP/CCD showed that EP/10 % CCD passed a UL-94 V-0 rating and possessed a LOI value of 31.6 %, which is 7.6 % higher than that of the neat EP. TGA results showed that the introduction of CCD into EP reduced the initial decomposition temperature. The results of the cone calorimeter test indicated that the release of heat was restrained significantly by CCD. Furthermore, the introduction of CCD decreased the total smoke product by 72 %. In order to investigate the flame-retardant mechanism of EP/CCD, XPS, FTIR, SEM and Raman were utilized to detect the char residue of EP/CCD, and its results indicated that CCD did possess a positive role in condensed-phase. In the respects of circular economy and environmental protection, flame retardants produced from chitosan was promising.

Acknowledgments

This work was financially supported by Hubei provincial science and technology department (2018ACA158)

References

Buczko, A., Stelzig, T., Bommer, L., Rentsch, D., & Heneczkowski, M. (2014). Bridged DOPO derivatives as flame retardants for PA6. *Polymer Degradation and Stability, 107*, 158–165.

Dong, L. P., Deng, C., Li, R. M., Cao, Z. J., & Lin, L. (2016). Poly(piperazinyl phosphamide): A novel highly efficient charring agent for an EVA/APP intumescent flame retardant system. *Royal Society of Chemistry Advances, 6*, 30436–30444.

Dong, L. P., Deng, C., & Wang, Y. Z. (2017). Influence of small difference in structure of polyamide charring agents on their flame-retardant efficiency in EVA. *Polymer Degradation and Stability, 135*, 130–139.

Gao, M., & Yang, S. S. (2010). A novel intumescent flame-retardant epoxy resins system. *Journal of Applied Polymer Science, 115*, 2346–2351.

Jian, R. K., Wang, P., Xia, L., Yu, X. Q., & Zheng, X. L. (2017). Low-flammability epoxy resins with improved mechanical properties using a Lewis base based on phosphaphenanthrene and 2-aminothiazole. *Journal of Materials Science, 52*, 9907–9921.

Jin, S. L., Qian, L. J., Qiu, Y., Chen, Y. J., & Xin, F. (2019). High-efficiency flame retardant behavior of bi-DOPO compound with hydroxyl group on epoxy resin. *Polymer Degradation and Stability, 166*, 334–352.

Liang, W. J., Zhao, B., Zhao, P. H., Zhang, C. Y., & Liu, Y. Q. (2017). Bisphenol-S bridged penta (anilino)cyclotriphosphazene and its application in epoxy resins: Synthesis, thermal degradation, and flame retardancy. *Polymer Degradation and Stability, 135*, 140–151.

Liu, X. D., Gu, X. Y., Sun, J., & Zhang, S. (2017). Preparation and characterization of chitosan derivatives and their application as flame retardants in thermoplastic polyurethane. *Carbohydrate Polymers, 167*, 356–363.

Mariappan, T., & Wilkie, C. A. (2014). Flame retardant epoxy resin for electrical and electronic applications. *Fire and Materials, 38*, 588–598.

Rakotomalala, M., Wagner, S., & Döring, M. (2010). Recent developments in halogen free flame retardants for epoxy resins for electrical and electronic applications. *Materials, 3*, 4300–4327.

Schartel, B., Balabanovich, A. I., Braun, U., Knoll, U., & Artner, J. (2007). Pyrolysis of epoxy resins and fire behavior of epoxy resin composites flame retarded with 9,10-dihydro-9-oxa-10-phosphaphenanthrene-10-oxide additives. *Journal of Applied Polymer Science, 104*, 2260–2269.

Shao, Z. B., Deng, C., Tan, Y., Chen, M. J., & Chen, L. (2014). An efficient mono-component polymeric intumescent flame retardant for polypropylene: Preparation and application. *ACS Applied Materials & Interfaces, 6*, 7363–7370.

Shen, D., Xu, Y. J., Long, J. W., Shi, X. H., & Chen, L. (2017). Epoxy resin flame-retarded via a novel melamine-organophosphinic acid salt: Thermal stability, flame retardance and pyrolysis behavior. *Journal of Analytical and Applied Pyrolysis, 128*, 54–63.

Tang, H., Zhu, Z. M., Chen, R., Wang, J. J., & Zhou, H. (2019). Synthesis of DOPO-based pyrazine derivative and its effect on flame retardancy and thermal stability of epoxy resin. *Polymers for Advanced Technologies, 30*, 2331–2339.

Wang, J. L., Ma, C., Wang, P. L., Qiu, S. L., & Cai, W. (2018). Ultra-low phosphorus loading to achieve the superior flame retardancy of epoxy resin. *Polymer Degradation and Stability, 149*, 119–128.

Wang, X., Hu, Y., Song, L., Xing, W. Y., & Lu, H. D. (2011). Effect of a triazine ring containing charring agent on fire retardancy and thermal degradation of intumescent flame retardant epoxy resins. *Polymers for Advanced Technologies, 22*, 2480–2487.

Xiong, Y. Q., Jiang, Z. J., Xie, Y. Y., Zhang, X. Y., & Xu, W. J. (2013). Development of a DOPO-containing melamine epoxy hardeners and its thermal and flame-retardant properties of cured products. *Journal of Applied Polymer Science, 127*, 4352–4358.

Yang, K., Xu, M. J., & Li, B. (2013). Synthesis of N-ethyl triazine-piperazine copolymer and flame retardancy and water resistance of intumescent flame retardant polypropylene. *Polymer Degradation and Stability, 98*, 1397–1406.

Yang, S., Wang, J., Huo, S. Q., Cheng, L. F., & Wang, M. (2015). Preparation and flame retardancy of an intumescent flame-retardant epoxy resin system constructed by multiple flame-retardant compositions containing phosphorus and nitrogen heterocycle. *Polymer Degradation and Stability, 119*, 251–259.

Yang, S., Wang, J., Huo, S. Q., Wang, J. P., & Tang, Y. S. (2016). Synthesis of a phosphorus/ nitrogen-containing compound based on maleimide and cyclotriphosphazene and its flame-retardant mechanism on epoxy resin. *Polymer Degradation and Stability, 126*, 9–16.

Zang, L., Wagner, S., Ciesielski, M., Müller, P., & Döring, M. (2011). Novel star-shaped and hyperbranched phosphorus containing flame retardants in epoxy resins. *Polymers for Advanced Technologies, 22*, 1182–1191.

Zhao, W., Liu, J. P., Peng, H., Liao, J. Y., & Wang, X. J. (2015). Synthesis of a novel PEPA-substituted polyphosphoramide with high char residues and its performance as an intumescent flame retardant for epoxy resins. *Polymer Degradation and Stability, 118*, 120–129.

Zhao, X., Babu, H., Llorca, J., & Wang, D. (2016). Impact of halogen-free flame retardant with varied phosphorus chemical surrounding on the properties of diglycidyl ether of bisphenol-A type epoxy resin: Synthesis, fire behaviour, flame retardant mechanism and mechanical properties. *Royal Society of Chemistry Advances, 6*, 59226–59236.

Zhu, Z. M., Wang, L. X., Dong, L. P., Liao, W., & Wang, Y. Z. (2019). Influence of a novel P/N-containing oligomer on flame retardancy and thermal degradation of intumescent flame-retardant epoxy resin. *Polymer Degradation and Stability, 162*, 129–137.

Zhu, Z. M., Xu, Y. J., Liao, W., Xu, S. M., & Wang, Y. Z. (2017). Highly flame retardant expanded polystyrene foams from phosphorus-nitrogen-silicon synergistic adhesives. *Industrial & Engineering Chemistry Research, 56*, 4649–4658.